Available online at www.sciencedirect.com
ScienceDirect
Proceedings of the Combustion Institute 000 (2018) 1–9
Proceedings of the Combustion Institute
www.elsevier.com/locate/proci

Self-sustained combustion of carbon monoxide over $CuCe_{0.75}Zr_{0.25}O_{\delta}$ catalyst: Stability operation and reaction mechanism

Feng Bin [a,*], Running Kang [a,b], Xiaolin Wei [a,b], Qinglan Hao [c], Baojuan Dou [c,*]

[a] *State Key Laboratory of High-Temperature Gas Dynamics, Institute of Mechanics, Chinese Academy of Sciences, Beijing 100190, PR China*
[b] *School of Engineering Science, University of Chinese Academy of Sciences, Beijing100049, PR China*
[c] *Tianjin University of Science & Technology, Tianjin 300457, PR China*

Received 28 November 2017; accepted 25 May 2018
Available online xxx

Abstract

The self-sustained combustion of carbon monoxide (CO) has been studied over the $CuCe_{0.75}Zr_{0.25}O_{\delta}$ catalyst by sol–gel method, and compared with the $CuCe_{0.75}Zr_{0.25}O_{\delta}$(H) and $Ce_{0.75}Zr_{0.25}O_{\delta}$ to investigate sensitivity of different active sites, such as dispersed CuO, Cu–Ce and Ce–Zr solid solution. The $CuCe_{0.75}Zr_{0.25}O_{\delta}$(H) is obtained via $CuCe_{0.75}Zr_{0.25}O_{\delta}$ sonicated in nitric acid to remove surficial CuO species, and the $Ce_{0.75}Zr_{0.25}O_{\delta}$ is prepared as the reference catalyst. Using the temperature programmed oxidation of CO together with an infrared camera (CO-TPO + FLIR), the catalytic activity for CO self-sustained combustion is determined not only by the ignition temperatures, following the decreasing order $CuCe_{0.75}Zr_{0.25}O_{\delta}$ (81 °C) > $CuCe_{0.75}Zr_{0.25}O_{\delta}$(H) (131 °C) > $Ce_{0.75}Zr_{0.25}O_{\delta}$ (167 °C) at the flow rate of 200 mL/min, but also by corresponding limits of lean combustion (equivalence ratio Φ) of 0.06–0.09, 0.10–0.13, 0.24–0.37, respectively, under the flow rate of 100–1000 mL/min. The M-K mechanism, in which adsorbed CO reacts with lattice oxygen, is crucial for all the catalysts via temperature programmed surficial reaction and in situ infrared analysis (TPSR + DRIFT). The sensitivity of active sites as follows: well-dispersed CuO > Cu–Ce solid solution > Ce–Zr solid solution. As rate-determining step for CO self-sustained combustion, CO is preferentially adsorbed on surficial dispersed CuO to yield carbonyls, and then the carbonyls interact with lattice oxygen to form CO_2 release. CO is secondly adsorbed on the surficial oxygen of copper and cerium sites in solid solution to yield carbonates. The carbonates formed are more stable and thus CO_2 is produced at the

* Corresponding authors.
E-mail addresses: binfeng@imech.ac.cn (F. Bin), bjdou@tust.edu.cn (B. Dou).

https://doi.org/10.1016/j.proci.2018.05.114

Please cite this article as: F. Bin et al., Self-sustained combustion of carbon monoxide over $CuCe_{0.75}Zr_{0.25}O_{\delta}$ catalyst: Stability operation and reaction mechanism, Proceedings of the Combustion Institute (2018), https://doi.org/10.1016/j.proci.2018.05.114

lower rate than carbonyls, indicating that the solid solution is less active than dispersed CuO. Exposed Ce^{3+} favors to form vacancies on the Cu–Ce solid solution surface, which is beneficial to adsorbing both CO and O_2, thus presenting the higher activity than Ce–Zr solid solution.

Keywords: $CuCe_{0.75}Zr_{0.25}O_\delta$; Carbon monoxide; Self-sustained combustion; Stability; Reaction mechanism

1. Introduction

The off-gas produced along with steelmaking contains tremendous amount of CO. Because the mixture of CO and O_2 tends to cause explosions, the off-gas yielded at steelmaking intermissions is not recovered directly as fuel, but is often discharged into the atmosphere via methane combustion-supporting flare burners [1]. To conserve the chemical heat that could have been discharged, our previous study found that the self-sustained catalytic combustion can be carried out via CO→CO_2 exothermic reaction [2], which not only lowers the auto ignition temperature in air as flameless combustion, but enables the burn-out of CO/air mixtures outside the explosion limits from diluted fuel streams. Considering the concentration/flow fluctuation of off-gas varying periodically along with the tap-to-tap cycle, extending the stability limits of catalytic combustion are essential in developing active catalysts to design robust combustion systems.

The mixed oxides containing copper, cerium and zirconium with solid solution structure are recognized as the most active media for CO oxidation among non-noble metal-based catalysts. Several surficial reaction models for CO oxidation, including details such as active sites and reaction pathways, have been proposed. Jia et al. [3] suggested that the surficial CuO species and Cu–Ce solid solution involves the activity, as the former provides sites for CO chemisorption and the latter promotes reducibility for oxygen activation. Gamarra and Martínez-Arias [4] found that CO chemisorption takes place to yield Cu^+-carbonyls, which are easily converted to CO_2. It is established, however, that CeO_2 provides active sites for CO and O_2 chemisorption to form carbonate species. The activation of CO also occurs over CeO_2 surface through either surficial coordinately unsaturated oxygen or surficial lattice oxygen anions, which both are surficial active oxygen species [5]. ZrO_2 cannot contribute to the activity directly, but it has been proposed that the addition of ZrO_2 (to form Ce–Zr solid solution) conduces to shape structural defects due to substitution of Ce^{4+} by Zr^{4+}, thus further enhances the oxygen mobility through the lattice, redox property, and sintering-resistant of CeO_2 [6]. Despite previous researches concerning reaction models for CO oxidation, the contributions of CuO species, solid solution types, oxygen vacancies to the catalytic activity and the predominant contributor to the enhanced activity are still not clear.

The catalytic ignition, as an unavoidable step of self-sustained catalytic combustion, has both scientific and applied interest. It is crucial for the understanding of catalytic surficial reactions to process safety and startup of complete oxidation systems. To investigate the ignition process of different fuels, many researches devoted to measuring the temperature accurately at which either surface or surface-initiated gas phase ignition occurs. FTIR and mass spectrometry are usually employed to detect gas phase products after reaction. Several studies have also focused on numerical modeling about ignition, considering the surficial chemistry, gas phase chemistry and transport processes [7]. Nevertheless, little statistical evidence related to the surficial species change during ignition has been reported yet. Based on the $CuCe_{0.75}Zr_{0.25}O_\delta$ catalyst, the present study tries to investigate the sensitivities of different active sites to the CO self-sustained catalytic combustion, combined with ignition temperature, self-sustained combustion limit, conversion efficiency, the wall temperature and heat output. Particularly, the chemisorption, active sites of the reactants and the reaction pathways were studied via temperature programmed surficial reaction (TPSR) and in situ infrared (DRIFT) analysis. These results obtained will bring new insights into the determinant factors and reaction mechanisms of CO self-sustained catalytic combustion.

2. Experimental specifications

2.1. Synthesis of catalysts

The $CuCe_{0.75}Zr_{0.25}O_\delta$ catalyst was prepared by sol–gel method, using $Cu(NO_3)_2{\cdot}3H_2O$, $Ce(NO_3)_3{\cdot}6H_2O$ and $Zr(NO_3)_4{\cdot}5H_2O$. This Cu:Ce:Zr molar ratio of 4:3:1 was selected according to structure optimization published by our previous work [8]. To investigate the contribution of well-dispersed CuO active sites to CO oxidation, partial $CuCe_{0.75}Zr_{0.25}O_\delta$ catalysts ($CuCe_{0.75}Zr_{0.25}O_\delta$ (H)) were sonicated in nitric acid to remove surficial CuO species. To compare the influence of different solid solutions on CO

Please cite this article as: F. Bin et al., Self-sustained combustion of carbon monoxide over $CuCe_{0.75}Zr_{0.25}O_\delta$ catalyst: Stability operation and reaction mechanism, Proceedings of the Combustion Institute (2018), https://doi.org/10.1016/j.proci.2018.05.114

oxidation, the $Ce_{0.75}Zr_{0.25}O_{\delta}$ reference catalyst with Ce:Zr molar ratio of 3:1 was prepared according to the same procedure for $CuCe_{0.75}Zr_{0.25}O_{\delta}$. These synthesis details of the catalysts are provided in the supporting information.

2.2. Characterization

X-ray powder diffraction (XRD) analysis was performed on an XD-3-automatic (PERSEE) equipped with a Cu Kα radiation source. For the elemental compositions of catalysts, X-ray fluorescence (XRF) analysis was obtained via a Power 4200 scanning XRF spectrometer. The morphology of catalysts was acquired from transmission electron microscope (TEM, PHILIPS Tecnai G^2 F20) observations. Raman spectra with the excitation laser at 488 nm were collected by a HORIBA LabRAM HR Evolution. X-ray photoelectron spectroscopy (XPS) was determined on a Kratos Axis Ultra DLD spectrometer. Temperature-programmed H_2 reduction (H_2-TPR) experiments were performed using a PCA-140 chemisorption analyzer (Builder) with 5% H_2/Ar at a heating rate of 10 °C/min to 800 °C. The TPSR was also conducted on the PCA-140 analyzer under the N_2 flow of 100 mL/min with a heating rate of 2 °C/min. Before TPSR, the catalyst was pretreated with N_2 at 300 °C and pre-adsorbed with 50%CO/N_2 at room temperature. A gas chromatograph (Shimadzu 2014B) was used for on-line monitoring of effluent gases. The DRIFT transmission spectroscopy was collected by a Bruker Tensor 27 spectrophotometer. Prior to recording spectra, the self-supporting sample disk was pretreated in the N_2 flow at 500 °C.

2.3. CO self-sustained catalytic combustion

CO catalytic combustion test was evaluated in a flow-type, temperature-controlled apparatus for continuous operation. The catalyst (200 mg, 0.1–0.15 mm in particle size) was loaded into a fixed-bed quartz tube reactor with an inner diameter of 4 mm. The flow rates of CO, O_2 and N_2 were controlled by mass flow controllers with a full-scale measurement accuracy of ± 1%. Temperature-programmed catalytic ignition of CO was performed under heating (5 °C/min) from room temperature in the CO/air mixture until the ignition temperature was reached, and a K thermocouple was located between the reactor wall and oven wall to control the oven temperature. The temperature distributions on the reactor surface were acquired by an infrared camera (FLIR T640) with a measurement accuracy of ± 2%. An online FTIR measurement system (QGS-08, Maihak) was employed to monitor the effluent CO, O_2 and CO_2.

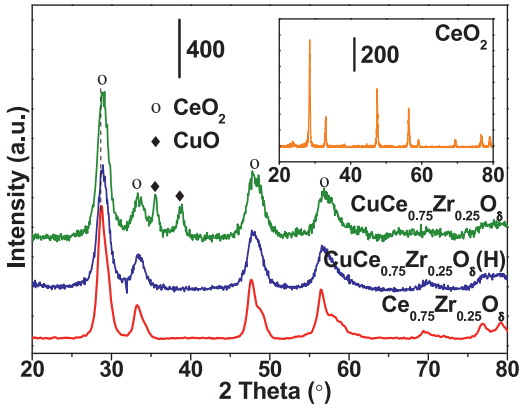

Fig. 1. XRD patterns of catalysts.

3. Results and discussion

3.1. Structure and morphology

Figure 1 shows the XRD patterns of the $CuCe_{0.75}Zr_{0.25}O_{\delta}$, $CuCe_{0.75}Zr_{0.25}O_{\delta}$(H) and $Ce_{0.75}Zr_{0.25}O_{\delta}$ catalysts. All the catalysts feature diffraction peaks of cubic CeO_2 with fluorite structure (PDF No. 34-0394). CuO phase is detected in the $CuCe_{0.75}Zr_{0.25}O_{\delta}$ but not observed in the $CuCe_{0.75}Zr_{0.25}O_{\delta}$(H), indicating that either the bulk CuO is removed or the crystallite size is below the detection limit of XRD after nitric acid treatment. Compared with pure CeO_2, the diffraction peak shifting toward higher 2θ value for the $CuCe_{0.75}Zr_{0.25}O_{\delta}$, $CuCe_{0.75}Zr_{0.25}O_{\delta}$(H) and $Ce_{0.75}Zr_{0.25}O_{\delta}$, reveal the incorporation of Cu and Zr into the CeO_2 lattice. The representative TEM images of catalysts are presented in Fig. 2. Except for Ce–Zr solid solution, the Cu–Ce solid solution and crystalline CuO is also observed in the $CuCe_{0.75}Zr_{0.25}O_{\delta}$ (Fig. 2A) by measuring the D-spacing (dCu–Ce solid solution (111) = 0.3125 nm and dCuO (111) = 0.2381 nm), and the former is smaller than dCe–Zr solid solution (111) = 0.3149 nm for the $Ce_{0.75}Zr_{0.25}O_{\delta}$ reference (Fig. 2C). Owing to the nitric acid treatment, CuO particles are not observed in the $CuCe_{0.75}Zr_{0.25}O_{\delta}$(H) (Fig. 2B), in agreement with XRD analysis.

3.2. Raman, XRF and XPS analysis

Figure 3 shows the Raman spectra of the catalysts. The spectrum of pure CeO_2 shows a main band around 463 cm^{-1}, which is related to the F_{2g} symmetry vibration mode of cubic fluorite-type structure. The two weak bands around 290 and 628 cm^{-1} are attributed to the evolution of oxygen vacancies from solid solutions, whereas the weak band at 1188 cm^{-1} is ascribed to the primary A_{1g} asymmetry of CeO_2. Based on the ratio between

Please cite this article as: F. Bin et al., Self-sustained combustion of carbon monoxide over $CuCe_{0.75}Zr_{0.25}O_{\delta}$ catalyst: Stability operation and reaction mechanism, Proceedings of the Combustion Institute (2018), https://doi.org/10.1016/j.proci.2018.05.114

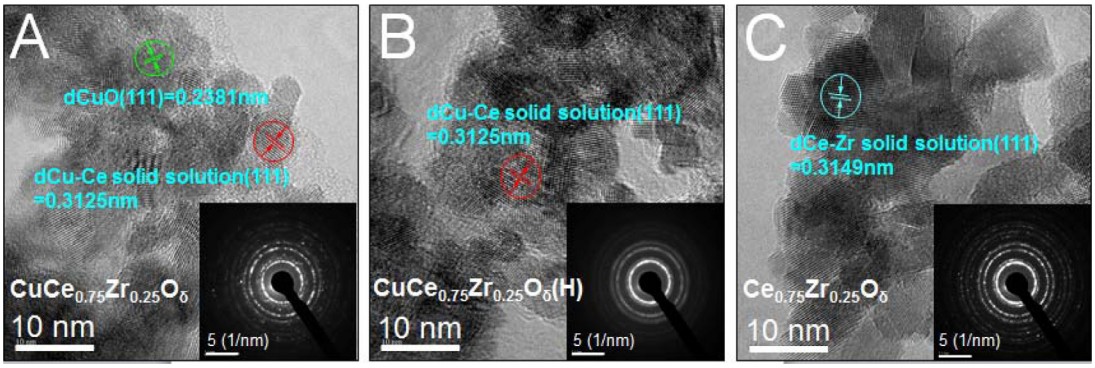

Fig. 2. TEM images of catalysts.

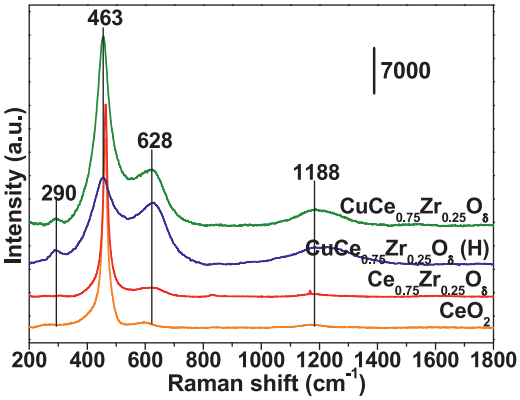

Fig. 3. Raman spectra of catalysts.

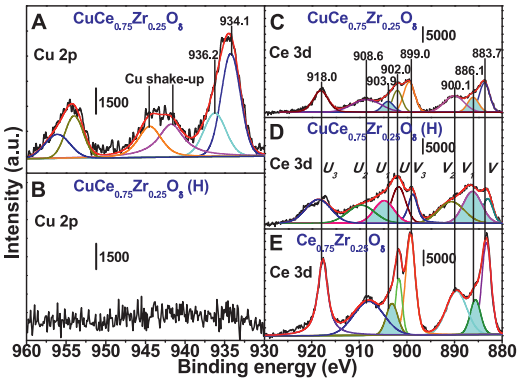

Fig. 4. XPS narrow spectra Cu 2p and Ce 3d over the catalysts.

the areas of peaks at 628 and 463 cm^{-1} (A_{628}/A_{463}), the concentration of surficial oxygen vacancies is analyzed semi-quantitatively for these catalysts, following the order of $CuCe_{0.75}Zr_{0.25}O_{\delta}$(H) (0.518) > $CuCe_{0.75}Zr_{0.25}O_{\delta}$ (0.402) > $Ce_{0.75}Zr_{0.25}O_{\delta}$ (0.287) > CeO_2 (0.04). It may be that the cerium substituted by zirconium and/or copper promotes the formation of oxygen vacancies, and the copper is more effective.

The chemical states and surficial compositions of catalysts are investigated by XPS. The Cu 2p spectrum (Fig. 4A) for the $CuCe_{0.75}Zr_{0.25}O_{\delta}$ shows two main peaks for Cu $2p_{3/2}$ and Cu $2p_{1/2}$ located at about 941.5 and 944.2 eV, and the shake-up peaks at 938.2–947.9 eV. The Cu $2p_{3/2}$ curve is fitted with two peaks corresponding to Cu^{+} (934.1 eV) and Cu^{2+} (936.2 eV), respectively, with the Cu^{2+}/Cu^{+} quantitative ratio of 0.65. The Cu 2p peak cannot be observed in $CuCe_{0.75}Zr_{0.25}O_{\delta}$(H) (Fig. 4B), however, which is attributed to surficial dispersed and crystallized CuO removed after nitric acid treatment. The XRF data confirm that the copper oxides exist in $CuCe_{0.75}Zr_{0.25}O_{\delta}$ at 33.38% but remain at only 4.32% in $CuCe_{0.75}Zr_{0.25}O_{\delta}$(H), indicating that the residual copper ions are incorporated into the CeO_2 lattice to form Cu–Ce solid solution. The Ce 3d spectra of the catalysts (Fig. 4C–E) are deconvoluted into $3d_{5/2}$ and $3d_{3/2}$ spin-orbit components (labeled v and u, respectively), arising from Ce^{4+} (v, v_2, v_3, u, u_2, and u_3)↔ Ce^{3+} (v_1 and u_1) electronic transitions. Quantitative data give Ce^{3+}/Ce^{4+} ratios of 0.15 for $CuCe_{0.75}Zr_{0.25}O_{\delta}$, 0.38 for $CuCe_{0.75}Zr_{0.25}O_{\delta}$(H) and 0.12 for $Ce_{0.75}Zr_{0.25}O_{\delta}$, respectively. The presence of Ce^{3+} in the catalysts favors to form vacancies and unsaturated chemical bonds on the catalyst surface [9].

3.3. H_2-TPR analysis

The redox properties of catalysts are analyzed by H_2-TPR, as shown in Fig. 5. The reduction temperature of the $Ce_{0.75}Zr_{0.25}O_{\delta}$ catalysts is within the range of 400–700 °C arising from poor redox properties of the ceria species. The $CuCe_{0.75}Zr_{0.25}O_{\delta}$ exhibits three reduction peaks at 100–300 °C, labeled α (165 °C), β (209 °C), γ (232 °C), which are correlated with the reduction of the copper

Please cite this article as: F. Bin et al., Self-sustained combustion of carbon monoxide over $CuCe_{0.75}Zr_{0.25}O_{\delta}$ catalyst: Stability operation and reaction mechanism, Proceedings of the Combustion Institute (2018), https://doi.org/10.1016/j.proci.2018.05.114

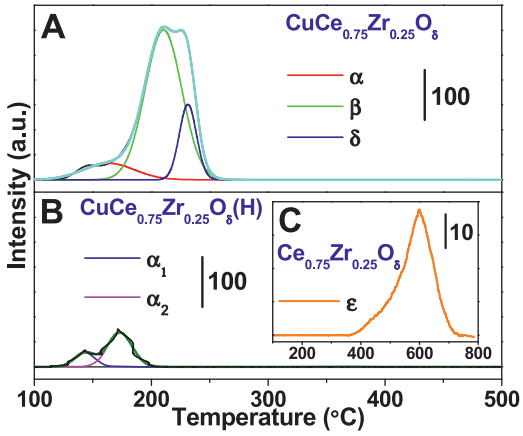

Fig. 5. H_2-TPR profiles of the catalysts.

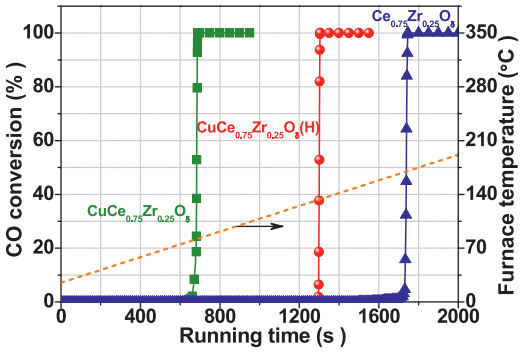

Fig. 6. Ignition curves of CO under different catalysts.

species in Cu–Ce solid solution, dispersed and crystallized CuO over $CuCe_{0.75}Zr_{0.25}O_\delta$ surface, respectively. Except α (α_1 and α_2), both β and γ peaks disappear in $CuCe_{0.75}Zr_{0.25}O_\delta$(H) because the surficial CuO is removed. Hence the redox properties of copper species decrease according to the reduction temperature following the order: Cu–Ce solid solution > dispersed CuO > crystallized CuO.

3.4. Temperature-programmed catalytic ignition of CO

Figure 6 reports the transient curves of CO ignition under the 15%CO/air atmosphere and total flow rate of 200 mL/min, following three main steps under the heating feed condition. Take the $Ce_{0.75}Zr_{0.25}O_\delta$ for instance, the first step can be described as a slow induction process that begins at 150 °C and then continues, at a relatively slow rate until 165 °C. Here the reaction is kinetically controlled, reflected by the temperature of catalyst bed close to the controlled temperature. The second step is the ignition process taking place at gas–solid phase interface, and the reaction rate is

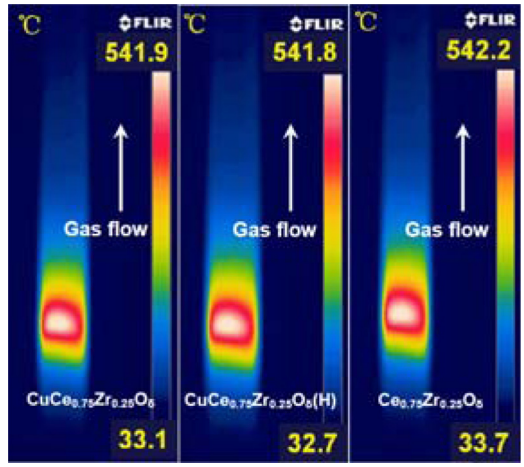

Fig. 7. Temperature fields in reactor for CO self-sustained catalytic combustion.

controlled by internal diffusion. the CO oxidation rate is fast enough to induce a strong increase of the local temperature which consequently accelerates the external diffusion and mass-transfer, on account of the gas diffusivity $D_v \propto T^{1.81}$ and the mass-transfer coefficient $K_s = (D_v \cdot S)^{1/2}$, where T denotes temperature and S denotes update frequency, respectively [10]. The third phase concerns temperatures well above the ignition region. Entering this step means the reaction rate becomes controlled by external diffusion [11]. The reaction activity for the CO catalytic ignition process follows the order $CuCe_{0.75}Zr_{0.25}O_\delta$ > $CuCe_{0.75}Zr_{0.25}O_\delta$(H) > $Ce_{0.75}Zr_{0.25}O_\delta$, corresponding to the ignition temperature (defined as the temperature at 30% CO conversion) of 81 °C, 131 °C, 167 °C, respectively. Figure 7 displays temperature fields in reactor for CO self-sustained catalytic combustion. The heat and mass movement during catalytic combustion occurs since the packed bed is cooled at the walls. The centerline tends to be hotter than the walls, reaction is faster, and reactants are more rapidly consumed there. When the self-sustained combustion is maintained, temperature gradients formed are mainly determined by gas composition rather than types of catalysts. The durability test of the catalyst has also been carried out. The self-sustained combustion of CO over the $CuCe_{0.75}Zr_{0.25}O_\delta$ can be maintained for 100 h with no deactivation of the catalyst, since no obvious difference of the high-temperature combustion region between the catalysts before and after durability experiments can be observed.

3.5. Stability limit of CO self-sustained catalytic combustion

Figure 8 displays the profiles of the equivalence ratios (Φ) limits of CO self-sustained combustion

Please cite this article as: F. Bin et al., Self-sustained combustion of carbon monoxide over $CuCe_{0.75}Zr_{0.25}O_\delta$ catalyst: Stability operation and reaction mechanism, Proceedings of the Combustion Institute (2018), https://doi.org/10.1016/j.proci.2018.05.114

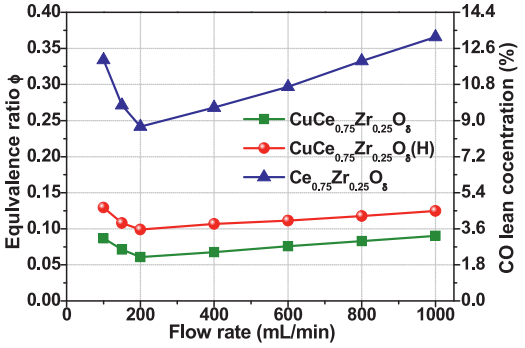

Fig. 8. Φ limits of CO self-sustained combustion at CO lean conditions.

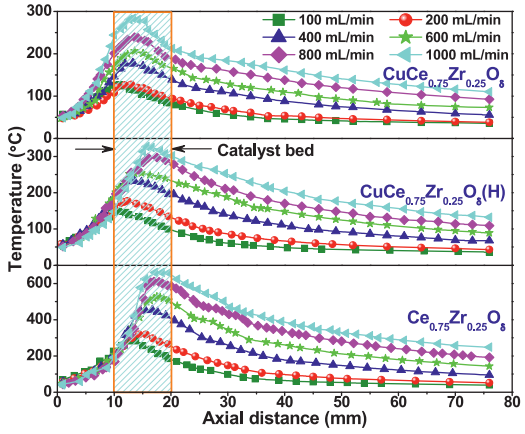

Fig. 9. The axial wall temperature along the combustion chamber.

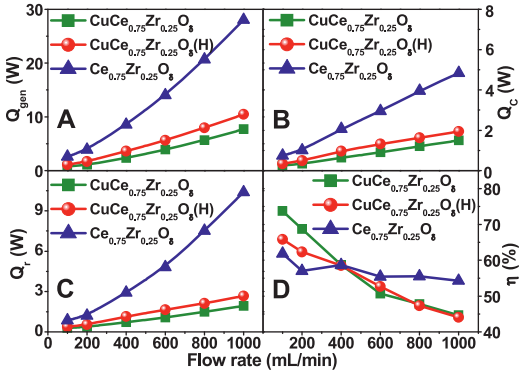

Fig. 10. The heat transfer versus flow rate over the catalysts.

at CO lean conditions. Here Φ is defined by CO to oxygen ratio in feed gas divided by the stoichiometric ratio for CO complete combustion. The effect of flow rate to Φ value is not a simple one. There is a local minimum near 200 mL/min, after which Φ value actually increases with flow rate. Obviously, the flow rate is too low to achieve self-combustion with oxygen enrichment, while high gas flow can blow out the hot points on catalyst surface due to heat loss under the same Φ value. Under the same flow rate, the Φ value of different catalysts is related to their activities (ignition temperature) and decreases following the order: $Ce_{0.75}Zr_{0.25}O_{\delta}$ > $CuCe_{0.75}Zr_{0.25}O_{\delta}(H)$ > $CuCe_{0.75}Zr_{0.25}O_{\delta}$. With respect to the self-sustained combustion of CO, the CO/oxygen mixture is first catalyzed to generate local hot spots on the catalyst surface. Because the rate of heat generation far exceeds the rate of heat loss to the surroundings, such exothermic chemical reactions of CO oxidation and resultant temperature rise, leading to catalytic ignition. Under the same flow rate, the catalyst with lower activity needs the higher stoichiometric ratio in order to afford the higher local temperature for the CO ignition, and thus a higher stability limit Φ is required.

The axial wall temperature along the reactor is measured over all the catalysts (Fig. 9). Here, the equivalence ratios for the lines in Fig. 9 are determined according to the limits of self-sustained combustion listed in Fig. 8. The high-temperature region is located at the axial distance 10–20 mm that corresponds exactly to the position of packed catalyst bed. This region shifts right slightly with the flow rate increasing for each catalyst, particularly the $CuCe_{0.75}Zr_{0.25}O_{\delta}(H)$ and $Ce_{0.75}Zr_{0.25}O_{\delta}$, since inadequate active sites per unit of catalysts are provided for CO combustion. The length of the catalyst bed has much effect on the limit of CO self-sustained combustion. For the $CuCe_{0.75}Zr_{0.25}O_{\delta}$, most of CO can be oxidized rapidly due to the fast mass transfer and thus releases lots of heat, enough to maintain the self-sustained combustion in the front of the catalyst bed, never needing to react along the gas flow. Thus the Φ limit has low sensitivity to the catalyst-bed length for the catalyst with high activity. By comparison, the less active $Ce_{0.75}Zr_{0.25}O_{\delta}$ needs the higher temperature to ignite CO, which should be accumulated in catalyst bed along the gas flow. The shorter catalyst-bed length should be compensated by the higher Φ limit in order to reach the ignition temperature in this case. The maximum of wall temperature for the $CuCe_{0.75}Zr_{0.25}O_{\delta}$ and $CuCe_{0.75}Zr_{0.25}O_{\delta}$ (H) is not up to 300 °C and 350 °C respectively during CO self-sustained combustion, lower than that of $Ce_{0.75}Zr_{0.25}O_{\delta}$ catalyst. The effect of both flow rate and Φ value is apparent: the Φ value should be enhanced with increasing the flow rate so that the enhancement of heat release can effectively offsets the heat transfer loss.

The balance of heat transfer is maintained during steady self-sustained combustion. Based on the data listed in Fig. 10, the heat transfer loss between the outer walls and ambient is calculated according

Please cite this article as: F. Bin et al., Self-sustained combustion of carbon monoxide over $CuCe_{0.75}Zr_{0.25}O_{\delta}$ catalyst: Stability operation and reaction mechanism, Proceedings of the Combustion Institute (2018), https://doi.org/10.1016/j.proci.2018.05.114

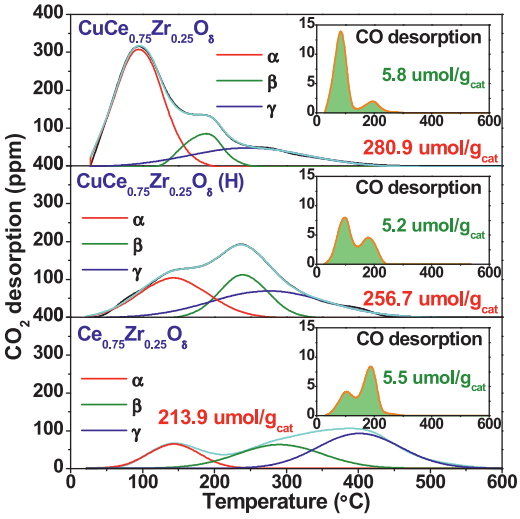

Fig. 11. TPSR profiles of CO and CO_2 desorption after the CO pre-adsorption.

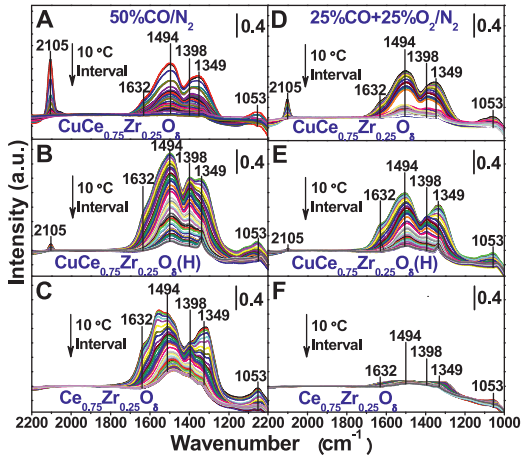

Fig. 12. DRIFT spectra for the CO oxidation (30–500 °C) under pre-adsorption conditions. The lines at several particular temperatures are displayed in Fig. S2 of the Supplemental material.

to the literature [12], and provided detailedly in the supporting information. From Fig. 10A–C, the total heat release (Q_{gen}), free convection heat transfer rate (Q_c) and radiation heat transfer rate (Q_r) exhibit the upward trend upon increasing the flow rate. As a result of high Φ value over $Ce_{0.75}Zr_{0.25}O_\delta$ catalyst, however, the corresponding values of Q_{gen}, Q_c, and Q_r are higher than that of $CuCe_{0.75}Zr_{0.25}O_\delta$ and $CuCe_{0.75}Zr_{0.25}O_\delta$(H). It can be observed that the Q_r value is slightly higher than Q_c under the same flow rate over the $CuCe_{0.75}Zr_{0.25}O_\delta$ and $CuCe_{0.75}Zr_{0.25}O_\delta$(H), while this distinction between Q_r and Q_c tends to be obvious over the $Ce_{0.75}Zr_{0.25}O_\delta$ at the flow rate ≥ 400 mL/min, relevant to its higher wall temperature (T_w, see Fig. 9) at CO self-combustion state ($Q_r \propto T_w^4$). Hence the surface heat loss rate per unit of generate power (η) over $Ce_{0.75}Zr_{0.25}O_\delta$ is also higher than that of $CuCe_{0.75}Zr_{0.25}O_\delta$ and $CuCe_{0.75}Zr_{0.25}O_\delta$(H) at the flow rate ≥ 400 mL/min. As expected, intensive luminous zones is observed in photographs because of thermal radiation within $Ce_{0.75}Zr_{0.25}O_\delta$ catalyst, given in Fig. S1 of the Supporting information.

3.6. TPSR analysis

Both TPSR and DRIFT analysis have been employed to investigate the intermediate active species during CO combustion. According to TPSR results presented in Fig. 11, the majority of adsorbed CO desorbs as CO_2 (280.9 μmol/g_{cat} for $CuCe_{0.75}Zr_{0.25}O_\delta$, 256.7 μmol/$g_{cat}$ for $CuCe_{0.75}Zr_{0.25}O_\delta$(H), and 213.9 μmol/$g_{cat}$ for $Ce_{0.75}Zr_{0.25}O_\delta$, respectively), but there is also trace desorption of CO (< 6 μmol/g_{cat}) at the temperature < 250°C. The CO_2 desorption for the $Ce_{0.75}Zr_{0.25}O_\delta$ starts immediately upon initiation of the temperature ramp, which is characterized by the α peak (145 °C), β peak (288 °C) and γ peak (402 °C), respectively. The CO_2 desorption peaks shift toward lower temperatures for the $CuCe_{0.75}Zr_{0.25}O_\delta$ and $CuCe_{0.75}Zr_{0.25}O_\delta$(H), especially the former, with a main peak located at 96 °C (α peak) and other two peaks at 140 °C (β peak) and 268 °C (γ peak), respectively. The shift and intensive peaks are associated with dispersed CuO and Cu–Ce solid solution formed which exhibit the higher redox ability than the Ce–Zr solid solution, in accordance with H_2-TPR results. This behavior can also be considered as an indication of enhancement of catalyst reactivity, because intermediate species are less stable so as to decompose at lower temperatures.

3.7. DRIFT analysis

To further demonstrate the intermediates in CO oxidation, DRIFT is firstly conducted under the N_2 flow of 100 mL/min with 10 °C/min heating rate. Before DRIFT, the catalyst is pretreated with N_2 at 300 °C, pre-adsorbed with 50%CO/N_2 or 25%CO + 25%O_2/N_2 and swept at 30 °C. Adsorption of 50%CO/N_2 on $CuCe_{0.75}Zr_{0.25}O_\delta$ (Fig. 12A) leads to form carbonyl bands (Cu^+–CO) at 2105 cm^{-1}, because d orbitals of copper ions are completely full. Three types of carbonates are still detected without gaseous oxygen during pre-adsorption, thanks to coordinative of CO to copper and cerium centers via surficial O atom in solid solution: bidentate carbonates (1053 cm^{-1}), monodentate carbonates (1349, 1398 and 1494 cm^{-1}) and bicarbonates (1632 cm^{-1}) [13]. With the temperature rising to 500 °C, the carbonyl peak falls

Please cite this article as: F. Bin et al., Self-sustained combustion of carbon monoxide over $CuCe_{0.75}Zr_{0.25}O_\delta$ catalyst: Stability operation and reaction mechanism, Proceedings of the Combustion Institute (2018), https://doi.org/10.1016/j.proci.2018.05.114

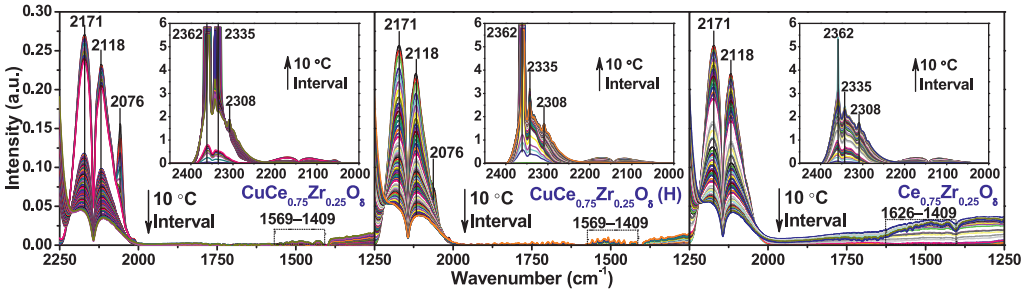

Fig. 13. DRIFT spectra for the CO oxidation (30–500 °C) under 5%CO + 25%O_2/N_2 continuous stream conditions. The lines at several particular temperatures are displayed in Fig. S3 of the Supplemental material.

rapidly, followed by decomposition of bicarbonates, bidentate and monodentate carbonates.

Similar spectra are observed for the $CuCe_{0.75}Zr_{0.25}O_\delta$(H) (Fig. 12B) and $Ce_{0.75}Zr_{0.25}O_\delta$ (Fig. 12C). However, the band at 2105 cm^{-1} is lost more over the $CuCe_{0.75}Zr_{0.25}O_\delta$(H) whereas disappears over the $Ce_{0.75}Zr_{0.25}O_\delta$ under 50%CO/N_2 pre-adsorption. The reasons are as follows: (1) Surficial CuO species have been removed after nitric acid treatment ($CuCe_{0.75}Zr_{0.25}O_\delta$(H)); (2) The Ce^{3+} and Ce^{4+}, with the outer shell electron distributions of 4f1 and 5S2 4d10 5P6, respectively, are difficult to offer electrons from D-orbitals to the anti-bonding π-orbitals of CO [14]. Due to the surficial CuO species removed and exposure of Ce^{3+} (confirmed by Raman and XPS analysis), the $CuCe_{0.75}Zr_{0.25}O_\delta$(H) (Cu–Ce solid solution) not only adsorbs more CO to form carbonates during pre-adsorption, but also is more active than those of $Ce_{0.75}Zr_{0.25}O_\delta$ (Ce–Zr solid solution) with the increase of temperature. These results provide evidence for TPSR analysis: the remarkable CO_2 desorption (α peak) at low temperatures can be mainly ascribed to decomposition of carbonyls over the $CuCe_{0.75}Zr_{0.25}O_\delta$ whereas the β and γ peaks are attributable to the decomposition of carbonates.

To investigate the interaction between CO and O_2 on catalysts, another similar DRIFT is performed under the 25%CO + 25%O_2/N_2 pre-adsorption conditions. As displayed in Fig. 12D–F, it should be stressed that the competitive adsorption between CO and O_2 on copper and cerium sites is apparent for each catalyst, in particular the cerium sites. Hence the peaks of carbonyls and carbonates are lower than those under 50%CO/N_2 pre-adsorption, where the carbonates formed on the $Ce_{0.75}Zr_{0.25}O_\delta$ are quite small.

The DRIFT is also carried out under the 5%CO + 25%O_2/N_2 continuous stream to identify main active sites during CO self-sustained catalytic combustion. The DRIFT spectra (Fig. 13) display intense bands at 2171 and 2118 cm^{-1} assigned to gaseous CO. Slight carbonate signals (1409–1626 cm^{-1}) can be observed, with the intensities descending in the order: $Ce_{0.75}Zr_{0.25}O_\delta$ > $CuCe_{0.75}Zr_{0.25}O_\delta$(H) > $CuCe_{0.75}Zr_{0.25}O_\delta$. The $CuCe_{0.75}Zr_{0.25}O_\delta$ exhibits a higher red-shifted peak of carbonyls (2076 cm^{-1}) [15] than the $CuCe_{0.75}Zr_{0.25}O_\delta$(H), which does not exist on the $Ce_{0.75}Zr_{0.25}O_\delta$. when the temperature increases from 30 to 500 °C, the CO band for the $CuCe_{0.75}Zr_{0.25}O_\delta$ reduces rapidly between 110 and 120 °C and the carbonyl band disappears, but the CO_2 bands at 2308, 2335 and 2362 cm^{-1} grow fast instead, confirming to reach self-sustained combustion. At this moment, all the carbonyls immediately convert to form CO_2 so that abundant copper sites can be renewed quickly. When the content of surficial CuO reduces, just as the $CuCe_{0.75}Zr_{0.25}O_\delta$(H) and $Ce_{0.75}Zr_{0.25}O_\delta$, moderate activities of Cu–Ce and Ce–Zr solid solutions are highlighted, corresponding the relative low yield of CO_2.

4. Conclusion

Self-sustained combustion of CO has been investigated over the $CuCe_{0.75}Zr_{0.25}O_\delta$ catalyst and compared with the $CuCe_{0.75}Zr_{0.25}O_\delta$(H) and $Ce_{0.75}Zr_{0.25}O_\delta$. The catalytic activity for CO self-sustained combustion decreases in the order: $CuCe_{0.75}Zr_{0.25}O_\delta$ > $CuCe_{0.75}Zr_{0.25}O_\delta$(H) > $Ce_{0.75}Zr_{0.25}O_\delta$, corresponding to the limits of lean combustion (Φ) of 0.06–0.09, 0.10–0.13, 0.24–0.37 respectively, within the flow rate of 100–1000 mL/min. Figure S4 illustrates the CO surface catalytic reaction pathways in the Supplemental material. The M-K mechanism, in which adsorbed CO reacts with lattice oxygen, is dominant for all the catalysts. The gas-phase oxygen is less important than lattice oxygen although the competitive adsorption between CO and O_2 is obvious. As rate-determining step for CO self-sustained combustion, CO is preferentially adsorbed on surficial dispersed CuO to yield carbonyls. Then the carbonyls interact with oxygen

Please cite this article as: F. Bin et al., Self-sustained combustion of carbon monoxide over $CuCe_{0.75}Zr_{0.25}O_\delta$ catalyst: Stability operation and reaction mechanism, Proceedings of the Combustion Institute (2018), https://doi.org/10.1016/j.proci.2018.05.114

atom bonded to a neighboring copper or cerium ions, forming the gaseous CO_2 release. The lattice oxygen consumed is supplemented by gas phase oxygen. CO is secondly adsorbed on the surficial oxygen of cerium sites in solid solutions to yield carbonates, in particular the Cu–Ce solid solution. The carbonates formed is so stable that CO_2 is produced at the lower rate than carbonyls, indicating that the Cu–Ce solid solution is less active than dispersed CuO although it exhibits excellent redox properties. Exposed Ce^{3+} on Cu–Ce solid solution favors to form vacancies and unsaturated chemical bonds on the surface, which is beneficial to adsorbing both CO and O_2, thus presenting the higher activity than Ce–Zr solid solution.

Acknowledgment

This work was supported by the National Natural Science Foundation of China (51776216, 51736010).

Supplementary materials

Supplementary material associated with this article can be found, in the online version, at doi:10.1016/j.proci.2018.05.114.

References

[1] S. Li, X. Wei, L. Yu, *Fuel* 90 (2011) 1350–1360.
[2] F. Bin, X. Wei, B. Li, K.S. Hui, *Appl. Catal. B: Environ.* 162 (2015) 282–288.
[3] A.P. Jia, G.S. Hu, L. Meng, Y.L. Xie, J.Q. Lu, M.F. Luo, *J. Catal.* 289 (2012) 199–209.
[4] D. Gamarra, A. Martínez-Arias, *J. Catal.* 263 (2009) 189–195.
[5] Y.N. Zheng, K.Z. Li, H. Wang, et al., *J. Catal.* 344 (2016) 365–377.
[6] O.H. Laguna, A. Pérez, M.A. Centeno, J.A. Odriozola, *Appl. Catal. B: Environ.* 176-177 (2015) 385–395.
[7] K. Maruta, *Proc. Combust. Inst.* 33 (2011) 125–150.
[8] S. Li, Q. Hao, R. Zhao, D. Liu, H. Duan, B. Dou, *Chem. Eng. J.* 71 (2013) 939–944.
[9] Q. Wan, L. Duan, K. He, J. Li, *Chem. Eng. J.* 170 (2011) 512–517.
[10] W.L. Mccabe, J.C. Smith, Peter Harriott, *Chem. Eng. Unit Oper.* 4 (1993) 527–565.
[11] P.A Carlsson, M. Skoglundh, *Appl. Catal. B: Environ.* 101 (2011) 669–675.
[12] J.P. Holman, *Heat Transfer*, The McGraw-Hill Companies, Inc, 2010.
[13] K.I. Hadjiivanov, G.N. Vayssilov, *Adv. Catal.* 47 (2002) 307–511.
[14] A. Hornés, P. Bera, A.L. Cámara, D. Gamarra, G. Munuera, A.M. Arias, *J. Catal.* 268 (2009) 367–375.
[15] I. Jbir, A. Paredes-Nunez, S. Khaddar-Zine, Z. Ksibir, *Appl. Catal. A: Gen.* 505 (2015) 309–318.

Please cite this article as: F. Bin et al., Self-sustained combustion of carbon monoxide over $CuCe_{0.75}Zr_{0.25}O_{\delta}$ catalyst: Stability operation and reaction mechanism, Proceedings of the Combustion Institute (2018), https://doi.org/10.1016/j.proci.2018.05.114